

The design of a laboratory facility for evaluating the structural response of small-diameter buried pipes

R.W.I. Brachman, I.D. Moore, and R.K. Rowe

Abstract: The design of a new laboratory facility for evaluating the structural response of small-diameter buried pipes (e.g., leachate collection pipes in landfills) is presented. The pipe is tested within a 2.0 m wide, 2.0 m long, and 1.6 m high prism of soil, subject to large vertical pressures (1000 kPa), with only minimal roughness and deflection of the lateral boundaries. Results from finite element analyses are presented to examine the effect of proximity, roughness, and stiffness of the lateral boundary on the soil and pipe response and how reasonable the laboratory idealizations are relative to the deep burial conditions expected to prevail in the field. Shear stresses arising from the roughness of the lateral boundaries alter the stresses acting around the pipe and reduce the proportion of the applied surcharge reaching the pipe. Outward deflection of the lateral boundaries also alters the stress state around the pipe, predominantly resulting from decreases in horizontal stresses within the soil. Reducing boundary friction to less than 5° and limiting the boundary deformation to less than 1 mm at a vertical surcharge of 1000 kPa provide a good idealization of field conditions for a deeply buried pipe.

Key words: buried pipes, soil–structure interaction, laboratory testing, boundary friction.

Résumé : On présente la conception d'une nouvelle installation pour évaluer la réaction structurale de petits tuyaux enfouis (e.g., tuyaux pour le captage de lixiviant dans les remblais sanitaires). Le tuyau est testé dans un prisme de sol de 2.0 m de largeur, 2.0 m de longueur, et 1.6 m de hauteur, soumis à de fortes pressions (1000 kPa) verticales, et confiné dans des frontières latérales ayant seulement un minimum de rugosité et de déflexion. On présente les résultats d'analyses en éléments finis pour examiner les effets de proximité, de rugosité et de rigidité des frontières latérales sur la réaction du sol et du tuyau, et pour déterminer à quel point sont raisonnables les idéalizations en laboratoire par rapport aux conditions d'enfouissement profond que l'on s'attend de trouver de façon prédominante sur le terrain. Les contraintes de cisaillement découlant de la rigidité des frontières latérales modifient les contraintes agissant autour du tuyau et réduisent la proportion de la surcharge appliquée qui atteint le tuyau. Une déflexion vers l'extérieur des frontières latérales modifie aussi l'état des contraintes autour du tuyau, résultant surtout de la diminution des contraintes horizontales à l'intérieur du sol. La réduction du frottement aux frontières à moins de 5° et la limitation de la déformation aux frontières à moins de 1 mm sous une surcharge verticale de 1000 kPa fournissent une bonne idéalisation des conditions sur le terrain pour un tuyau profondément enfoui.

Mots clés : tuyaux enfouis, interaction sol-structure, essai en laboratoire, frottement aux frontières.

[Traduit par la Rédaction]

Introduction

Large-scale testing of buried pipes is useful for evaluating the response of the soil and structure expected under field conditions. Such facilities include the test cells at Utah State University, University of Massachusetts at Amherst, and Ohio University in the United States; the University of Western Ontario in Canada; and LGA Geotechnical Institute in Germany.

As with most laboratory investigations, the boundary conditions of the testing apparatus may significantly influence the results derived from the test. The boundary conditions of the facilities for testing pipe include the method of load application and the geometry of the testing conditions. The state of stress in the soil around the pipe and, consequently, the structural response of the pipe may be significantly influenced by these boundary conditions.

Each of the existing facilities has limitations related to the boundary conditions in the facility. Both the Utah State and Ohio facilities attempt to simulate the deep burial response of a pipe. However, the Utah State cell essentially applies hydrostatic stress conditions to the soil around the pipe (Kastner et al. 1993) which differ from the biaxial stresses expected to occur in the field. Also, no effort is made to control friction that can mobilize along the side walls of the facility. The soil and pipe response when tested in the Ohio facility differs substantially from that expected to occur in a

Received June 1, 1998. Accepted August 16, 1999.

R.W.I. Brachman.¹ Department of Civil and Environmental Engineering, University of Alberta, Edmonton, AB T6G 2G7, Canada.

I.D. Moore and R.K. Rowe. Department of Civil and Environmental Engineering, The University of Western Ontario, London, ON N6A 5B9, Canada.

¹Author to whom all correspondence should be addressed.

typical field installation (Brachman et al. 1996). A complex response is produced because the overburden pressure is simulated by applying load through a stiff, rectangular plate.

Hoop compression cells at the University of Massachusetts (Selig et al. 1994) and the University of Western Ontario (Moore et al. 1996) provide a simple idealization of the pressures acting on the soil near a buried pipe by explicitly modelling the earth pressures as a uniform radial pressure. This considerably simplifies the laboratory conditions required for testing, yields results that are relatively straightforward to interpret, and provides a useful measure of pipe response under simplified soil pressures. The main shortcoming of this approach, however, is that the biaxial response (i.e., vertical pressures greater than horizontal pressures) that occurs in the field is not simulated by the axisymmetric applied radial pressure.

None of the existing facilities can closely approximate the expected field conditions with respect to the stress state associated with deep and extensive burial in a zone of soil surrounding a pipe. There is a need for a facility that would allow a laboratory assessment of the performance of small-diameter pipes under expected service conditions (e.g., a deeply buried leachate collection pipe in a landfill).

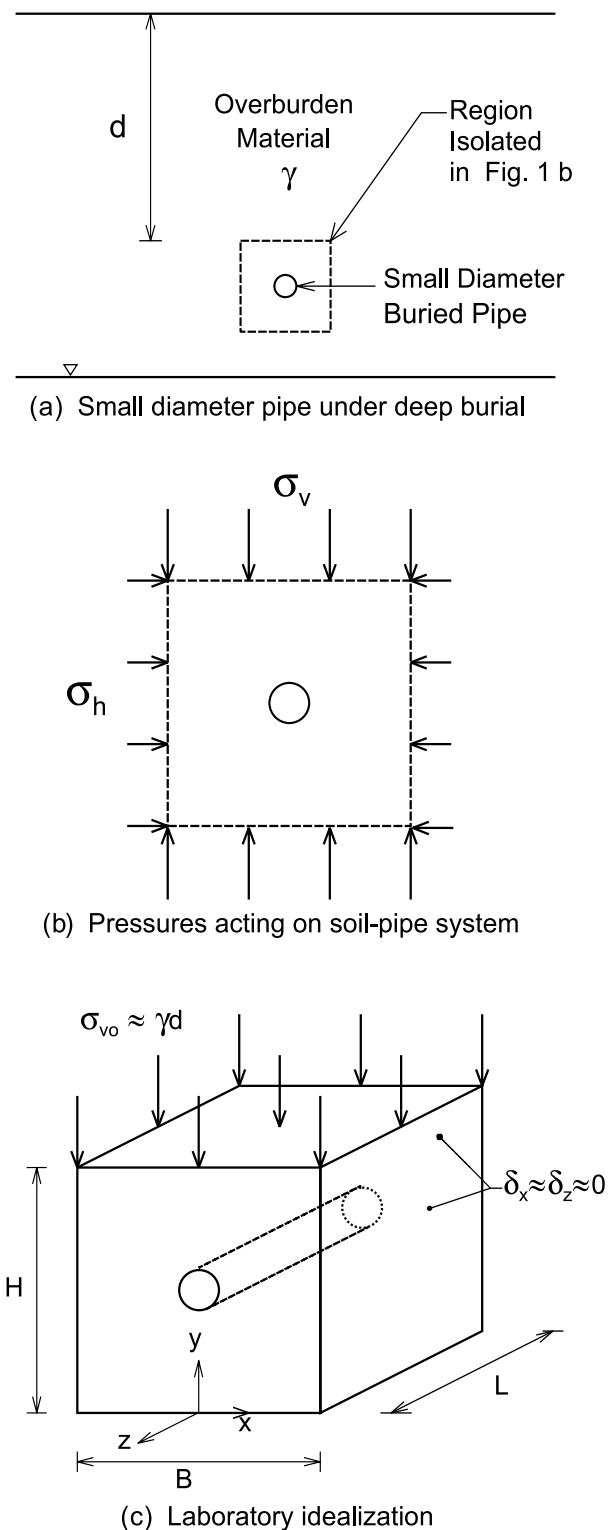
The objective of this paper is to discuss the design of a new laboratory facility for evaluating the performance of small-diameter pipes when buried under deep and extensive overburden material. The facility involves a prism of soil with a pipe buried within, subject to large vertical pressures while allowing only small horizontal deflections along the lateral boundaries. Attention is focussed on the influence of the boundary conditions in the new facility and how reasonably the test cell represents the field conditions for a buried pipe. Issues such as the loading conditions under deep burial, simulation of vertical earth pressures, development of lateral earth pressures, selection of test cell dimensions, and influence of side wall friction and boundary stiffness on soil and pipe response are examined.

Loading conditions under deep burial

The first step considered in the design of the laboratory facility involved identifying the boundary conditions experienced by the pipe when buried in the field. Figure 1a shows an idealized installation of a deeply buried small-diameter pipe. The pipe is typically surrounded by a select backfill material and is subjected to pressures from the overburden above. For example, these conditions could represent a pipe buried under an earth embankment or within a leachate collection system in a deep landfill. The buried pipe does not act as an isolated structural element with clearly defined applied loading, but rather as a component of the soil-pipe system. The structural performance of the pipe is a function of both the soil and pipe stiffness and the resulting soil-structure interaction. Consequently, to simulate the expected field conditions the soil-pipe system must be modelled in the laboratory.

A region of soil around the pipe is isolated in Fig. 1b showing idealized earth pressures acting distant from the pipe. Pressures arise at the boundaries of the soil-pipe system from deep burial. These pressures have a vertical component σ_v arising from the weight of the overlying materials

Fig. 1. Idealization of earth pressures acting on a region of soil around a deeply buried pipe.



above the pipe and a horizontal component σ_h associated with the restraint against lateral soil movement within the embankment. Horizontal stresses are often expressed as $K\sigma_v$, where K is the coefficient of lateral earth pressure. Provided that these biaxial stresses can be simulated in a

laboratory model, a reasonable idealization of field conditions should be attained.

Simulation of vertical earth pressure

The vertical stress from the weight of the overburden material may be reasonably represented by applying a uniformly distributed pressure σ_{vo} at the surface of the soil in the test cell (Fig. 1c). This pressure corresponds to some equivalent height of overburden material. For extensive and prismatic geometry, and where earth pressures are invariant in the horizontal direction, the applied pressure may be considered to be equivalent to the weight of the column of soil of height d per unit area (Fig. 1a). For other cases where overburden stresses vary in the horizontal direction, various analytical or numerical solutions may be employed to estimate the stresses in the vicinity of the pipe for a given embankment geometry.

The stiffness of the overburden above the backfill material used in the cell is neglected in this idealization. Burial under extensive and uniform stratigraphy does produce uniform vertical stresses at some distance above the pipe. Provided that the uniform stress boundary is placed sufficiently far above the pipe in the laboratory model (distance largely controlled by pipe diameter), a reasonable approximation for deeply buried pipes is obtained. Further, in some deep burial applications (e.g., landfills) most of the fill stiffness comes from the drainage stone placed around the pipe (which is present in the laboratory test) and the waste above this stone will typically be expected to have a much lower stiffness than the stone.

Conditions encountered by pipes buried within a trench could also be simulated in the new laboratory facility. In this case a proportion of overburden stress is attenuated by shear stresses mobilized along the sides of the trench. This paper, however, focuses only on the case of deep burial within extensive soil materials.

Other investigators have used a variety of approaches to attempt to simulate the earth pressures expected under deep burial. For example, both testing facilities at Utah State University and Ohio University use hydraulic cylinders to apply forces to steel plates that in turn apply pressures to the soil. At Utah State, many steel plates are used, whereas one large (1.83 m \times 2.74 m) platform is used in the Ohio facility. Finite element analysis of the Ohio University facility (Brachman et al. 1996) has shown that this method of load application gives rise to a complex stress state which is quite different to that expected in the field.

Another approach involves the use of pressurized bladders to apply a uniformly distributed pressure. This approach has been used by many investigators. Höeg (1968) appears to be the first to report the use of a vulcanized neoprene rubber bag to simulate large applied pressures. DiFrancesco et al. (1994) and Rogers et al. (1996) also used bladders but at much lower pressures (207–380 kPa and 150 kPa, respectively). Zanzinger and Gartung (1995, 1998) report on the use of water-filled flat jacks pressurized up to 1000 kPa.

Pressurized air bladders were selected to simulate the vertical stresses acting on the soil–pipe system. Several types of bladder construction were tried. The first involved seamed sheets of 1 mm thick, nylon-reinforced chlorosulphonated

polyethylene. This economical design was used for several tests (e.g., Brachman 1997; Moore and Laidlaw 1997; Brachman et al. 1998) and worked well for lower pressures ranging from 250 to 500 kPa. Rupture of these bladders at higher pressures resulted from material failure, usually near the edge seams. An alternative design using a diaphragm-type arrangement, involving a 3 mm thick Buna N rubber membrane with a mechanical seal around the perimeter (for details see Brachman 1999), proved more reliable, especially at high pressures, and was adopted for use in the new laboratory facility.

A maximum vertical surcharge of 1000 kPa was selected for the new facility. This pressure level corresponds to the deep burial case of roughly 50 m in an embankment soil (with unit weight $\gamma \approx 20$ kN/m³) or from 77 to 125 m in a municipal solid waste facility ($\gamma \approx 8$ –13 kN/m³), and was considered to cover most practical situations.

Simulation of lateral earth pressure

Horizontal stresses could be simulated in a similar manner by applying lateral pressures equivalent to the horizontal stresses σ_h generated in the field. Unfortunately the magnitude of the horizontal stress relative to the vertical stress (i.e., K) is not well defined for many backfill materials (it is a complex function of particle size, shape, gradation, density, and stress history). An alternate approach of controlling the displacement at the lateral boundary of the soil–pipe system was therefore adopted. Here, lateral stresses are developed by limiting the outward deflection of the side walls (i.e., by simulating $\delta_x \approx 0$ or K_o conditions, where K_o is the coefficient of lateral earth pressure at rest; Fig. 1c). Hence the soil will generate horizontal stresses close to those expected in the field for the backfill and lateral earth pressures conditions responding under zero lateral strain. To achieve this, the lateral boundary must be sufficiently stiff to minimize outward deformations of the soil and must be located far enough from the pipe so that the behaviour of the pipe is not significantly altered.

The boundary condition perpendicular to the pipe axis is also idealized as a small displacement boundary ($\delta_z \approx 0$ in Fig. 1c). Axial stresses σ_z will also develop at these boundaries in a manner similar to that of the horizontal stresses σ_x . Stiff side walls should reasonably represent the plane strain axial conditions of the pipe which would be expected to prevail for a long pipe buried in the field. Axial restraint conditions other than plane strain could also be simulated in the test cell.

Selection of test cell dimensions

Another important idealization of the field problem involved the selection of a finite region of the soil–pipe system for modelling in the laboratory. Two important issues controlled the selection of cell dimensions (i.e., breadth B , length L , and height H shown in Fig. 1c). First, it is recognized that the vertical and horizontal stresses in the embankment are disturbed locally around the pipe, since the pipe has different stiffness to that of the volume of soil it replaces. The proximity of the top surface of the cell must therefore be sufficiently remote from the pipe so that vertical

stresses are close to uniform. Similarly, the bottom surface of the cell must be sufficiently remote so that a stiff boundary does not induce nonuniform vertical stresses. The regions above and below a buried pipe where stress is attenuated are of approximately equal size and are controlled by the pipe diameter. Reasonable physical modelling of soil stresses is attained provided that the pipe is located no closer to the surface or the base than a distance equal to the pipe diameter.

Second, friction mobilized on the vertical side walls of the test cell is inevitable. Shear stresses acting on the lateral boundaries differ from those acting on the idealized soil block shown in Fig. 1*b*. Control of the roughness of the side walls is important to limit this effect. Furthermore, the side walls must be located far enough away from the pipe that most of the pressure applied to the top surface of the soil block reaches the pipe. This establishes a relationship between the pipe diameter and lateral test cell dimensions B and L .

The magnitude of interface friction mobilized in the laboratory test cell depends on the surface roughness of the side walls. For rough steel in contact with the soil, the ratio of the side wall interface friction angle to internal angle of friction of the soil (ϕ_{sw}/ϕ) may range from 0.8 to 0.9, whereas for smooth steel ϕ_{sw}/ϕ may be 0.5–0.7 (Perloff and Baron 1976). Consequently, for granular backfill materials with ϕ between 30° and 55° the friction angle for an untreated surface may vary from 15° to 50°.

The degree to which friction acts on the side walls may be reduced by treatment of the soil–steel interface. The need to reduce the friction on a boundary has been previously examined in other laboratory investigations. For example, Bathurst and Benjamin (1988) reported that side wall friction could be reduced to 15° by using sheets of polyethylene layered between sand and a Plexiglas side wall. Direct shear tests conducted to assess the effectiveness of different interface treatments (Tognon et al. 1999) found side wall friction angles ϕ_{sw} between 16° and 21° (depending on backfill soil) for minimal interface treatment (geotextile and polyethylene sheet), whereas 5° was found for layered polyethylene sheets lubricated with silicone grease.

An estimate of the proportion of the applied pressure that reaches the soil within the test cell can be obtained by modifying classical arching theory to consider the three-dimensional geometry of the laboratory test cell. The vertical stress at depth h below the surface in a cell of width B and length L , subjected to an applied surface pressure of σ_{vo} (Fig. 1*c*), can be estimated by

$$[1] \quad \sigma_v = \frac{\gamma}{2K\mu w} (1 - e^{-2K\mu wh}) + \sigma_{vo} e^{-2K\mu wh}$$

where

w is the geometry coefficient = $1/B + 1/L$;

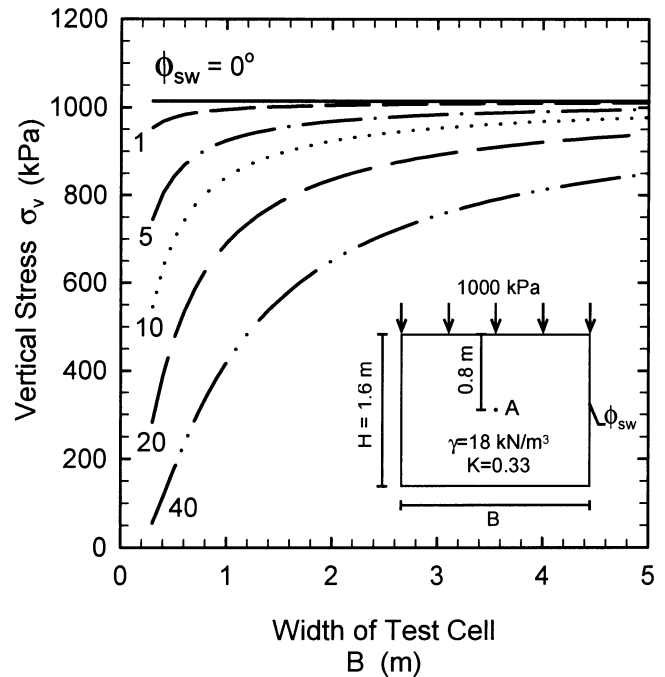
K is the coefficient of lateral pressure;

μ is the coefficient of side wall friction = $\tan \phi_{sw}$;

ϕ_{sw} is the angle of side wall friction; and

γ is the unit weight of the soil.

Fig. 2. Estimate of vertical stress at mid-depth (point A) for various levels of side wall friction ϕ_{sw} with increasing width B of the test cell when subject to 1000 kPa applied vertical pressure.



The vertical stress at mid-depth in the test cell calculated using eq. [1] is plotted in Fig. 2 for increasing width B of the test cell and for a range of interface friction angles ϕ_{sw} . Compressive stresses are taken as positive. The results shown are for the specific case of a square cell (i.e., $B = L$) of height 1.6 m (i.e., $h = 0.8$ m) with a pressure of 1000 kPa applied at the surface (also taking $\gamma = 18$ kN/m³ and $K = 0.33$).

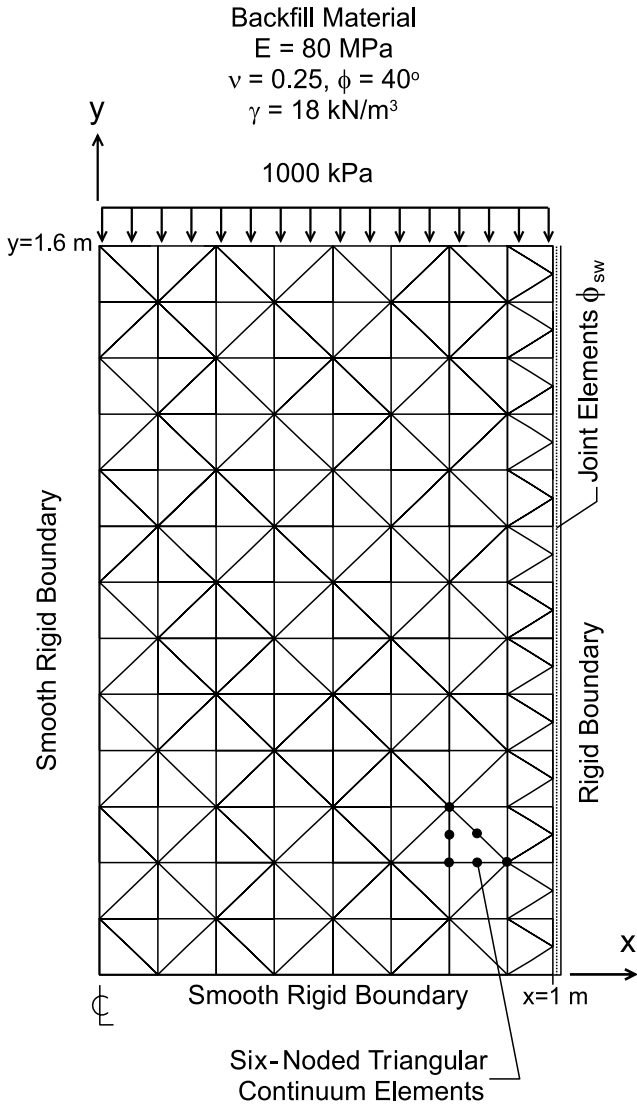
The results in Fig. 2 provide an initial estimate of the influence of the distance to the lateral boundary coupled with the effect of boundary roughness. As the distance to the boundary increases, the proportion of the vertical stress reaching mid-depth increases. Theoretically, if the boundary is sufficiently remote (i.e., for large values of B), there is negligible loss in applied pressure with depth. However, once B becomes sufficiently large, further increases result in only slight improvements in the stresses acting within the ground. With a test cell width B equal to 2 m, a good approximation is achieved for side wall friction angle of less than 10°, as 99, 95, and 91% of the applied vertical stress is calculated at this location for ϕ_{sw} of 1, 5, and 10°, respectively.

Based on the calculations from eq. [1] and also considering the cost of test cell fabrication (recognizing that larger dimensions involve stiffer side walls) and the logistics of test cell use (e.g., volume of soil required for testing), dimensions with height 1.6 m, breadth 2.0 m, and length 2.0 m were selected.

Influence of side wall friction on soil response

The simple arching model of eq. [1] provides a good indication of the significance of the proximity and roughness of

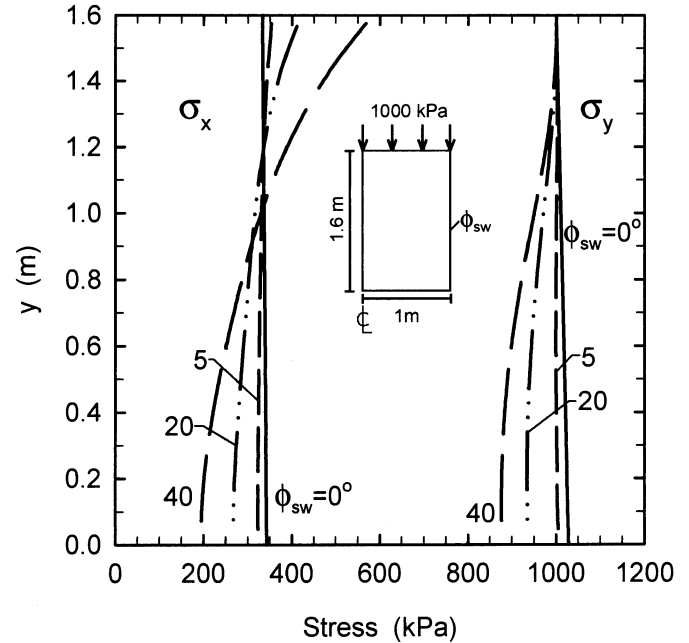
Fig. 3. Finite element mesh used to investigate soil – test cell interaction by considering half of a 2 m wide by 1.6 m high block of soil subject to vertical surcharge with interface friction ϕ_{sw} .



the lateral boundary. The results of finite element analysis of a test cell with the selected dimensions ($B = 2$ m) were studied to further investigate the effect of side wall friction and lateral stiffness on the soil and pipe response.

The case of the test cell backfilled only with a hypothetical soil material (Young's modulus $E = 80$ MPa, Poisson's ratio $\nu = 0.25$, angle of internal friction $\phi = 40^\circ$, angle of dilatancy $\psi = \phi/4$, cohesion $c = 0$, and unit weight $\gamma = 18$ kN/m³) was analyzed first to assess the stress redistribution within the soil for various levels of side wall friction. Two-dimensional, plane-strain, elastoplastic, finite element analysis with a Mohr-Coulomb failure criterion and the nonassociative flow rule of Davis (1969) was employed. The selection of soil modulus of 80 MPa (e.g., a well-compacted granular backfill) is considered to represent an upper bound for the ground materials likely to be tested in the new facility. Pore-water pressures are assumed to be zero for this assessment of boundary conditions.

Fig. 4. Vertical σ_y and horizontal σ_x stresses with depth along the test cell centreline subject to a vertical surcharge of 1000 kPa with different side wall friction values ϕ_{sw} .



The finite element mesh used for the analysis is shown in Fig. 3. Two hundred and seventy-four six-noded triangular continuum elements were used to model the soil. Symmetry along the centreline of the test cell was used. Side wall friction was simulated with 53 two-noded joint elements with interface friction angle ϕ_{sw} . The results were insensitive to the roughness of the bottom boundary, and consequently results are given with the base modelled as smooth and rigid.

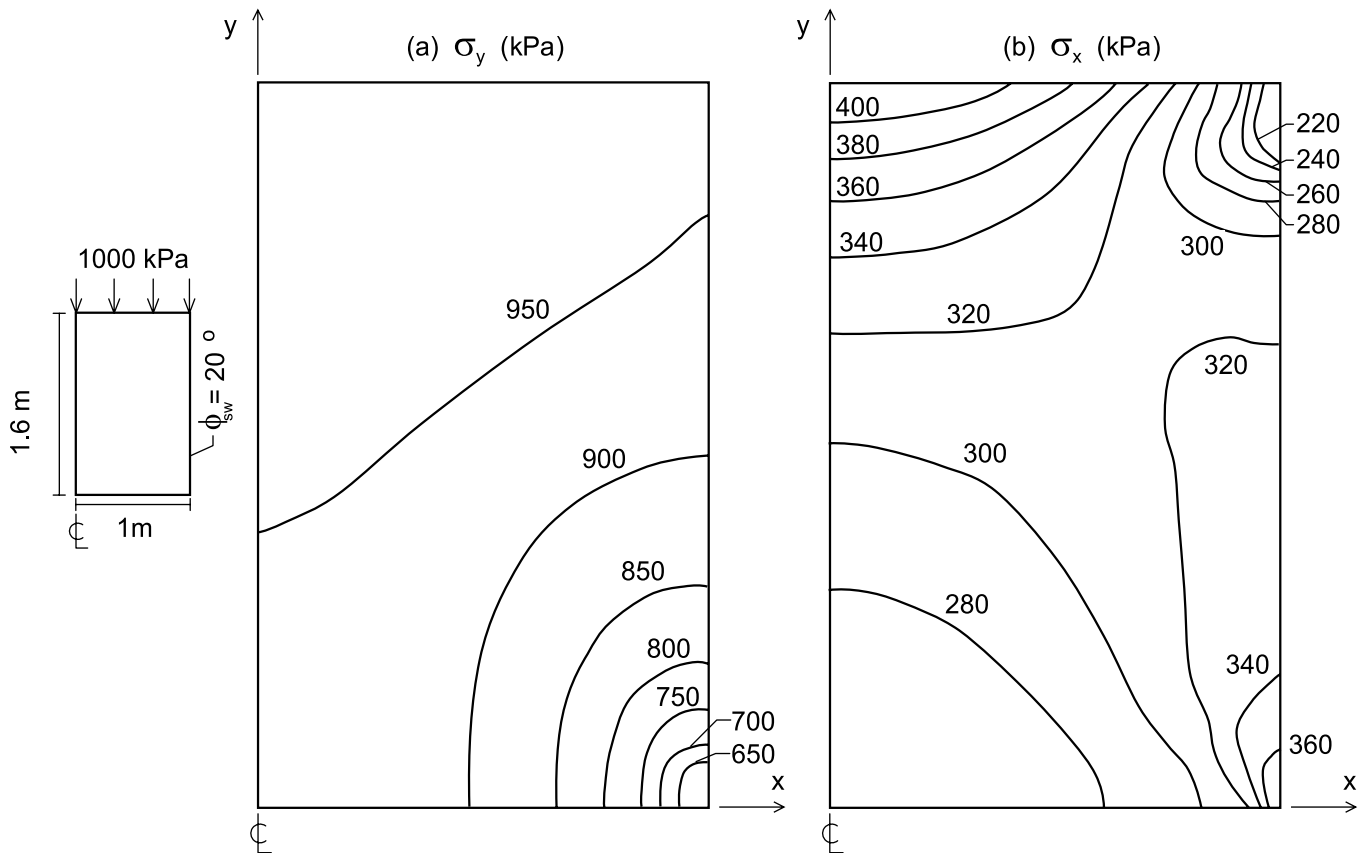
Figure 4 shows plots of vertical σ_y and horizontal σ_x stresses with depth near the centreline of the test cell for a 1000 kPa pressure uniformly applied across the surface. Results are shown for the limits of a smooth ($\phi_{sw} = 0^\circ$) and rough ($\phi_{sw} = \phi$) side wall, as well as two intermediate values of $\phi_{sw} = 5^\circ$ and 20° .

When the side walls are perfectly smooth ($\phi_{sw} = 0^\circ$), the stresses are uniform in the lateral direction (i.e., x) and increase linearly with depth because of the soil self-weight (i.e., $\sigma_y = \sigma_{vo} + \gamma h$, where $\sigma_{vo} = 1000$ kPa and h is the depth below the surface). At the surface ($y = 1.6$ m) the vertical stress is equal to the applied stress, 1000 kPa; at the base the vertical stress is equal to 1028.8 kPa. Horizontal stresses equal to $K\sigma_v$, where $K = \nu/(1 - \nu) = 0.33$, are developed. Real soil materials are expected to have other K values, but the results calculated here should still be a good indicator of the impact of the boundary condition.

The stress redistribution along the centreline caused by shear stresses mobilized along the side walls is evident from the other results presented in Fig. 4. As the angle of side wall friction increases, the vertical stresses decrease with depth. For example, at mid-depth ($y = 0.8$ m) the proportion of vertical stress relative to smooth side walls is 99, 94, and 87% for ϕ_{sw} of 5° , 20° , and 40° , respectively.

These values are slightly larger than those calculated using the modified arching theory from eq. [1] (e.g., 4% difference

Fig. 5. Vertical (a) and horizontal (b) stresses calculated for half of a 2 m wide by 1.6 m high block of soil subject to a vertical surcharge of 1000 kPa with interface friction ϕ_{sw} of 20° .



for ϕ_{sw} of 5°). The differences arise as the finite element analysis models arching in the x and y directions only, and thus overestimates the stress with depth relative to three-dimensional conditions. This difference will be minimal for interface friction angles of 5° . The modified arching solution, however, simplistically assumes full mobilization of the interface shear stresses and no rotation of principal stresses, whereas the finite element analysis models progressive shear mobilization along the interface and allows lateral redistribution of stresses, both of which are likely to occur in the laboratory facility. Thus despite the limitation imposed by using two-dimensional geometry, the finite element results provide a more reasonable assessment of the influence of side wall friction than does the modified arching solution.

Contours of vertical stress σ_y with ϕ_{sw} equal to 20° (associated with minimal surface treatment) are given in Fig. 5a. The transfer of stresses to the side wall is evident from the large decrease in σ_y , particularly near the side wall and close to the base of the cell where the vertical stresses reduce to 650 kPa.

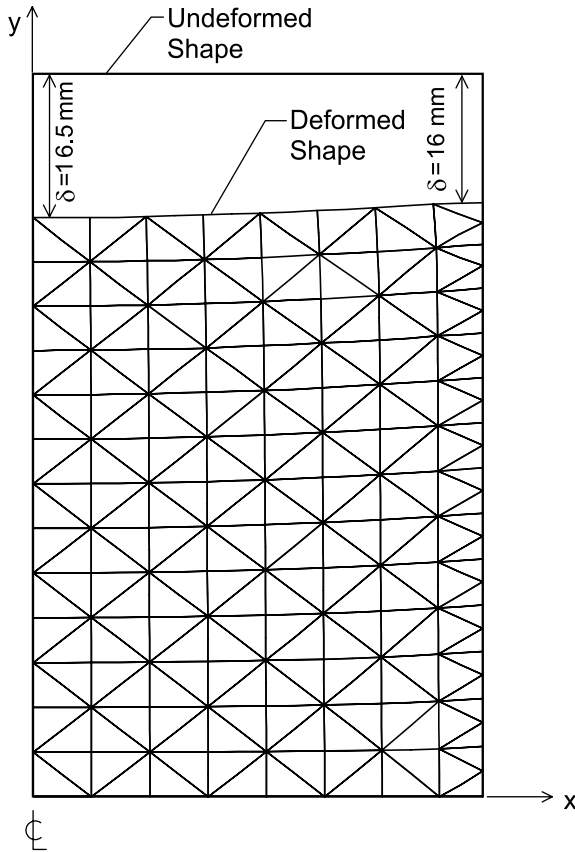
Horizontal stresses σ_x are also no longer uniform in the lateral direction and are not proportional to σ_y with one particular K value if shear stresses are allowed to develop along the side wall. Figure 4 shows that horizontal stresses along the centreline increase near the surface and then decrease with depth (relative to $\phi_{sw} = 0^\circ$) as ϕ_{sw} increases. At mid-depth there is 97%, 89%, and 85% of the horizontal stress with smooth side walls for ϕ_{sw} of 5° , 20° , and 40° .

Contours of horizontal stress σ_x are shown in Fig. 5b for ϕ_{sw} equal to 20° and appear to be quite complex. Close to the surface there are zones of increasing σ_x towards the centre of the test cell (also apparent in Fig. 4) and decreasing σ_x closer to the side wall (both relative to $\phi_{sw} = 0^\circ$). This stress distribution is attributed to the deformation of the soil mass (Fig. 6) as the soil near the centreline experiences greater compression in the horizontal direction. This effect becomes more pronounced for greater levels of friction mobilized along the interface (see Fig. 4). Close to the side wall and near the surface, lateral soil deformations are away from the boundary (i.e., towards the centre of the soil block), yielding smaller horizontal stresses.

At greater depths, the horizontal stress contours illustrate the transfer of stresses to the side walls. Associated with this redistribution are rotations of principal stresses. Figure 7 plots vectors of principal stress (σ_1 and σ_3 are major and minor principal stresses, respectively) for ϕ_{sw} equal to 20° . Also shown in Fig. 7 are contours of principal stress rotation α that refers to the counterclockwise rotation of the orientation of the major principal stress from the vertical. A maximum rotation of principal stresses of 12° occurs in the lower corner of the test cell.

Treatment of the lateral boundary with lubricated polyethylene sheets reduces side wall friction to less than 5° (Tognon et al. 1999). The vertical stress contours with ϕ_{sw} equal to 5° are plotted in Fig. 8a. Note that a much smaller contour interval of 20 kPa is used compared with the 50 kPa

Fig. 6. Deformed shape ($\times 20$) of half of a 2 m wide by 1.6 m high block of soil subject to a vertical surcharge of 1000 kPa with interface friction ϕ_{sw} of 20° .



contour interval of Fig. 5a. Less than 2% difference in vertical stresses occurs throughout most of the stress field. Vertical stresses are still somewhat reduced in the lower corner of the test cell (6% reduction); however, this region of soil is remote from the centre of the cell (i.e., location of the pipe).

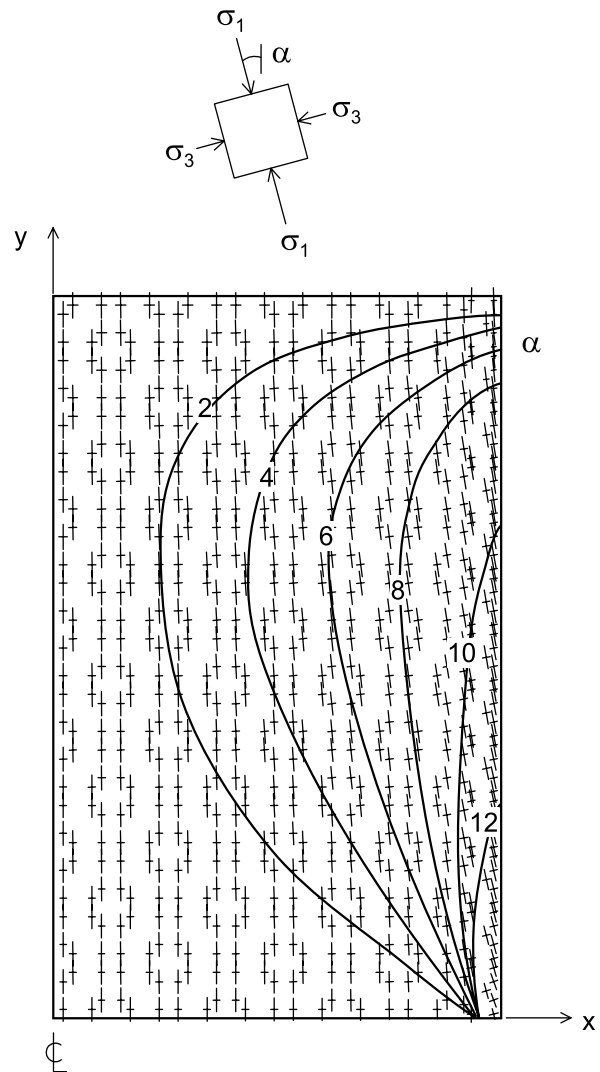
Horizontal stresses for ϕ_{sw} of 5° are plotted in Fig. 8b. Again a finer contour interval was used to illustrate the stress field. The pattern of horizontal stresses is similar to that with ϕ_{sw} equal to 20° , however the stress changes are substantially smaller for the lower interface friction angle of 5° . There is only a small (less than 3%) effect on stresses at mid-depth (i.e., pipe location). The rotation of principal stresses is substantially reduced for side wall friction of 5° (Fig. 9). Principal stress rotation is less than 1° for over half of the soil mass and is only 2° adjacent to the side wall.

Influence of side wall friction on soil and pipe response

The previous section illustrated the impact of side wall friction on the response of a block of soil within the test cell. The effect of side wall friction on a pipe buried within soil inside the test cell is now considered.

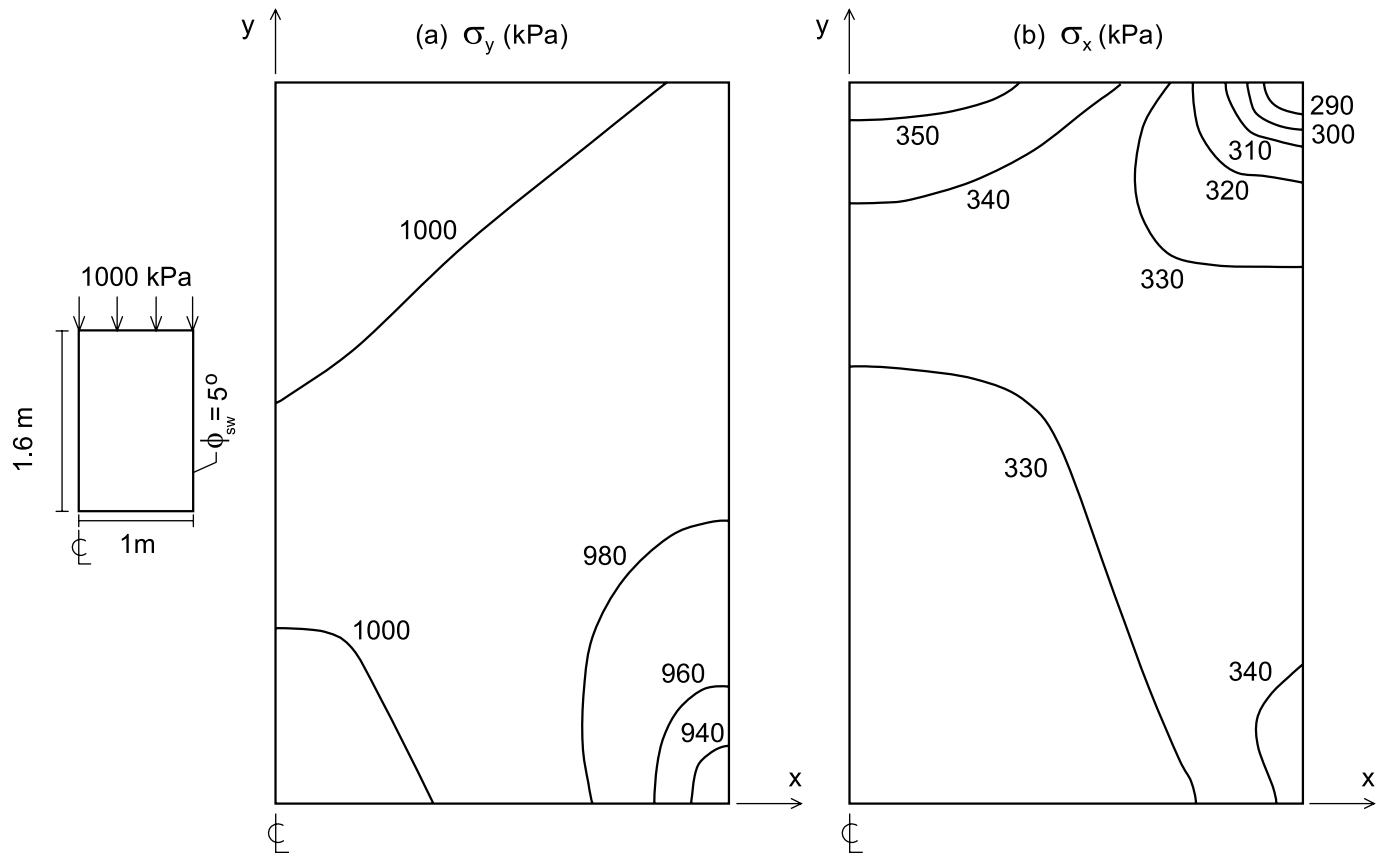
Figure 10 shows the finite element mesh used to assess the impact of cell boundaries on the soil stress distributions and the pipe response. The base boundary was again modelled as smooth and rigid, and the side walls as rigid with an

Fig. 7. Vectors of major σ_1 and minor σ_3 principal stress for half of a 2 m wide by 1.6 m high block of soil subject to a vertical surcharge of 1000 kPa with interface friction ϕ_{sw} of 20° . Also shown are contours of the rotation of major principal stress from the vertical (α) in degrees.



angle of surface friction ϕ_{sw} . Ninety-seven two-noded joint elements were used to model surface friction. The soil was modelled using 784 six-noded triangles, and 136 six-noded triangles were used to model the pipe. As in the previous section, the soil was modelled with modulus 80 MPa, Poisson's ratio 0.25, and internal angle of friction 40° . A high-density polyethylene pipe of outside diameter 320 mm and wall thickness 32 mm and located in the middle of the test cell was modelled with elastic modulus 500 MPa and Poisson's ratio 0.4. More sophisticated constitutive models are being used to characterize the response of plastic pipe (e.g., Moore and Hu 1995; Zhang and Moore 1997) but are not warranted in this preliminary assessment of pipe-soil-cell interaction. Plane strain analysis of the pipe-soil-cell system was undertaken which neglects the impact of wall friction and wall rigidity in the third dimension (along the pipe axis). Shear stresses along the interface between the soil and the pipe were limited by the friction angle ϕ of 40° .

Fig. 8. Vertical (a) and horizontal (b) stresses calculated for half of a 2 m wide by 1.6 m high block of soil subject to a vertical surcharge of 1000 kPa with interface friction ϕ_{sw} of 5° .



Soil stresses

Figure 11 shows the distribution of vertical stress σ_y and horizontal stress σ_x along a vertical section through the soil 0.2 m away from the pipe centreline. Solutions are given for side wall friction angles ϕ_{sw} of 0° , 5° , 10° , 24° , and 35° . These results are similar to those obtained for the cell filled with soil only (no pipe), but in addition to the stress redistribution because of friction on the lateral boundary there is a local perturbation in the stress field arising from the difference in stiffness of the pipe and volume of soil it replaces.

For small friction angles (less than or equal to 5°), the impact on stresses near the pipe is negligible. As expected, impact increases with depth, and for a friction angle associated with minimal surface treatment ($\sim 24^\circ$) the vertical stresses decrease by approximately 12% at the base of the cell. Stress decrease at the pipe location is roughly 6% for wall friction of 24° .

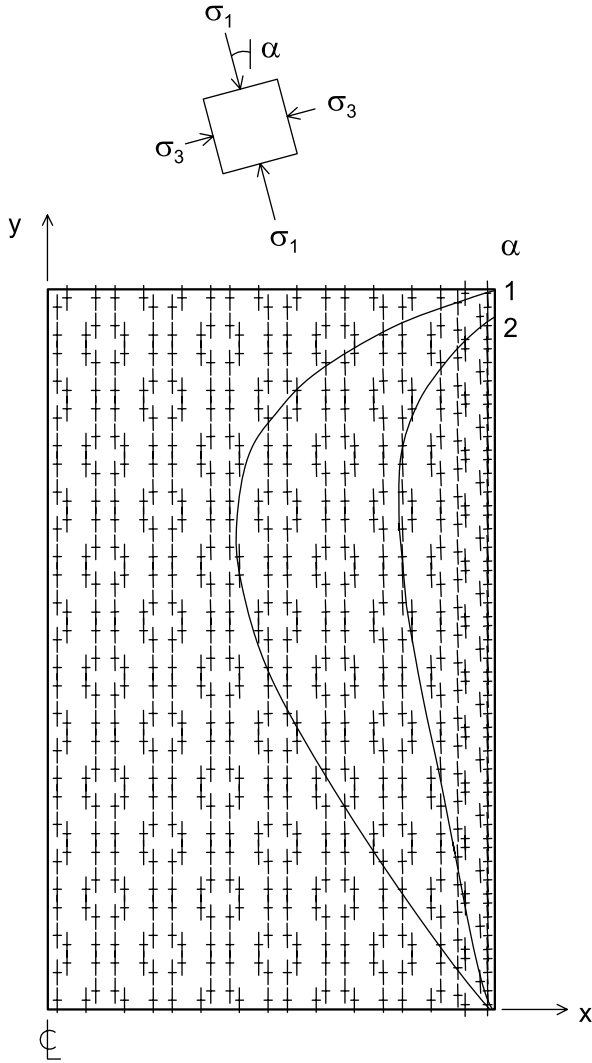
The impact of the pipe on stresses adjacent to the side wall (along $x = 0.925$ m) can be examined from the results in Fig. 12. For the case of smooth side walls ($\phi_{sw} = 0^\circ$), slight decreases in vertical stress and increases in horizontal stress towards mid-height ($y \approx 0.8$ m) occur relative to values with soil only in the cell (Fig. 4). These trends indicate that near this location (2.6 pipe diameters) away from the pipe, the impact of pipe on horizontal stresses is of the order of 10%, and less than 1% for vertical stresses (both relative to soil only in the cell). The magnitude of these changes will have a minimal influence on the overall soil-pipe response.

This indicates that the lateral boundary is located sufficiently far from the 320 mm diameter pipe. The proximity to the stiff side wall will become more important as pipe diameter increases. Pipes with diameters greater than 500 mm may be significantly affected by the proximity of the side wall.

As wall roughness increases, the vertical stress decreases with depth. For a high interface friction angle of 35° , roughly one third of the overburden stress reaches the cell base at this location adjacent to the wall. Wall friction also decreases the horizontal stress values towards the upper ground surface. This is similar to what is predicted if the pipe is absent, where the mode of ground deformation affects lateral stresses at this location. The impact for expected range of wall friction (5 – 24°) is clearly seen. These stress changes are related to the horizontal stress increases near the cell centreline close to the ground surface seen in Fig. 11 which are also largely independent of the pipe.

Figure 13 shows contours of vertical and horizontal stress in the ground with a side wall friction angle of 5° . The redistribution of stresses in the soil arising from the difference in the pipe stiffness compared with that of the volume of soil it replaces (i.e., arching) is evident. The vertical stress field of 1000 kPa (Fig. 13a) shows zones of both increasing and decreasing stress near the pipe. Vertical stresses decrease above the crown, below the invert, and directly adjacent to the spring line of the pipe. Zones of soil near the shoulder (between crown and spring line) and the haunch (between

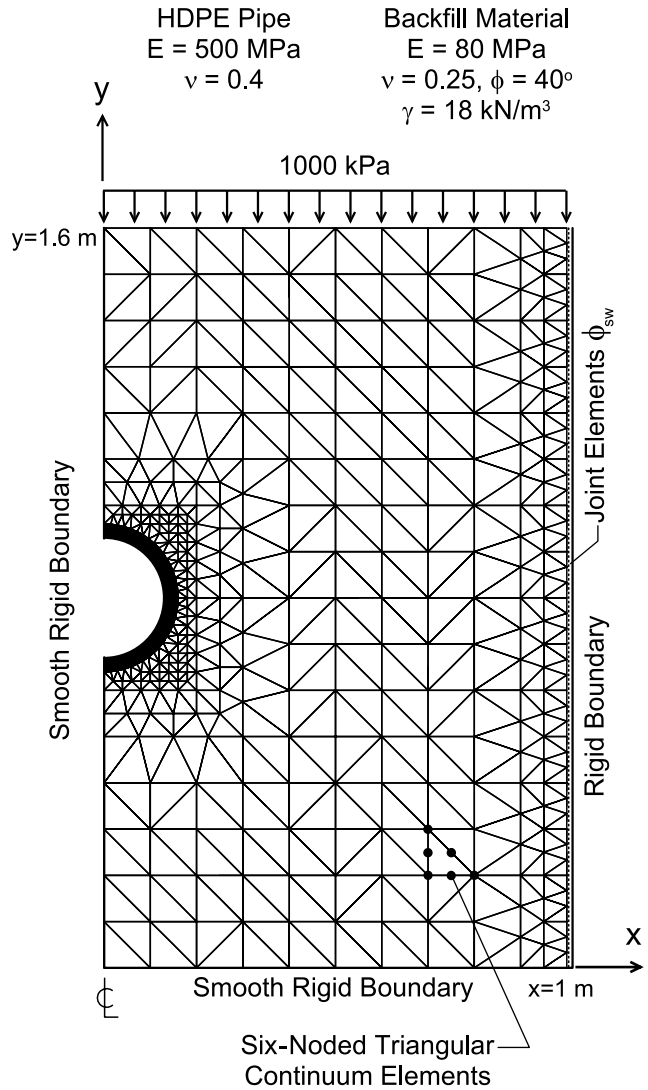
Fig. 9. Vectors of major σ_1 and minor σ_3 principal stress for half of a 2 m wide by 1.6 m high block of soil subject to a vertical surcharge of 1000 kPa with interface friction ϕ_{sw} of 5°. Also shown are contours of the rotation of major principal stress from the vertical (α) in degrees.



spring line and invert) of the pipe experience increases in vertical stress. The stress redistribution occurs largely within one pipe diameter away from the pipe, and the vertical and horizontal boundaries have little effect on the arching around the pipe. Horizontal stresses (Fig. 13b) increase above the crown, below the invert, and adjacent to the spring line. Regions of lower horizontal stress occur near the shoulder and haunch locations around the pipe.

Limits of soil arching (Moore 1993) exist for stiff pipes where the pipe attracts loads from the surrounding soil (negative arching) and flexible pipes where loads are shed to the surrounding soil (positive arching). This thick-wall polyethylene pipe experiences some positive arching (with ground stiffness $E = 80$ MPa and $\nu = 0.25$) but not to the extent of that for profile-wall polyethylene pipe (for the same soil stiffness) because of the larger hoop stiffness for the thick pipe.

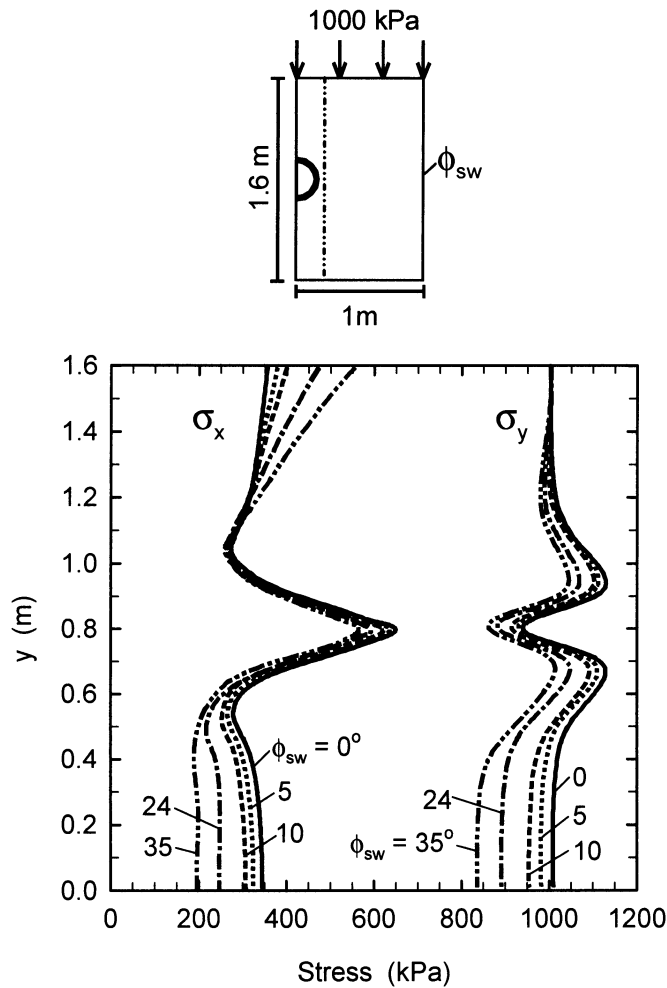
Fig. 10. Finite element mesh used to investigate soil – pipe – test cell interaction by considering half of a 2 m wide by 1.6 m high block of soil subject to a vertical surcharge with interface friction ϕ_{sw} and a 0.32 m outside diameter pipe (32 mm thick) centrally buried within the cell.



Pipe response

Side wall friction also has an impact on pipe deflections. The results from the finite element analysis are summarized in Table 1 for various side wall friction angles. Increases in ϕ_{sw} result in a decrease in magnitude of the vertical deflection at both the crown and the invert (δ_{cr} and δ_{in}) of the pipe because of reductions in the stresses that reach the pipe. The horizontal deflection at the spring line (δ_{sp}) of the pipe increases with greater boundary friction resulting from reduced lateral confinement provided to the pipe as stress is redistributed towards the side wall. For example, the magnitude of the vertical diameter change ($\Delta D_v = \delta_{cr} - \delta_{in}$) is 3% smaller for ϕ_{sw} of 24° compared with that for smooth side walls. The horizontal diameter change ($\Delta D_h = 2\delta_{sp}$) increases relative to smooth side walls by 8% for ϕ_{sw} equal to 24°. Overall, the pipe deflections are not greatly sensitive to

Fig. 11. Calculated vertical σ_y and horizontal σ_x stresses with depth 0.2 m away from the pipe centreline when subject to a vertical surcharge of 1000 kPa with different values of side wall friction ϕ_{sw} .



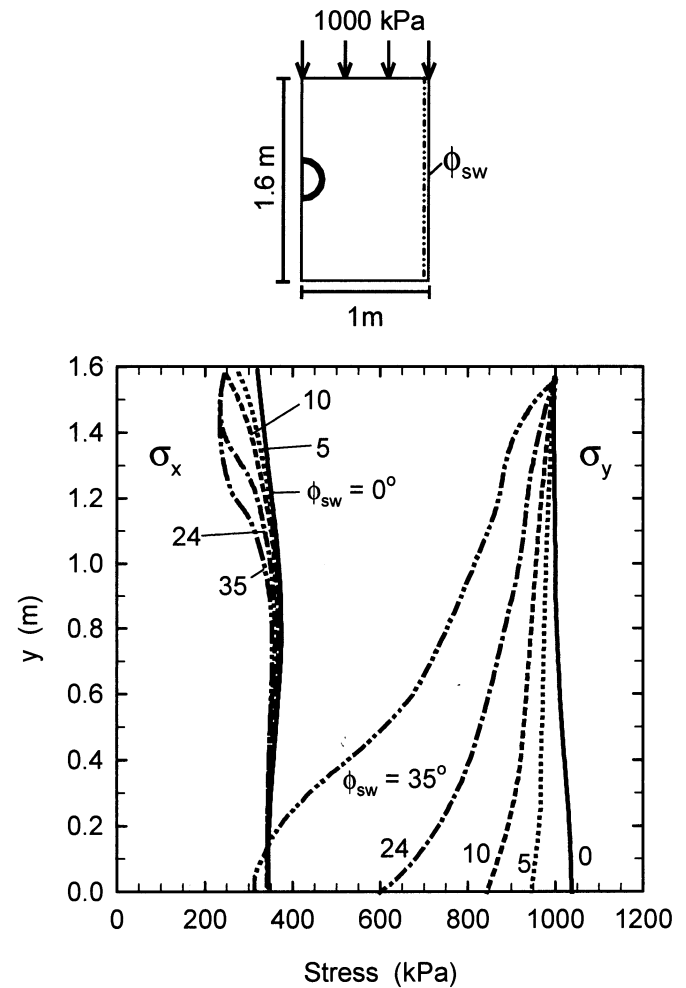
levels of side wall friction mobilized on the lateral boundaries.

The results from both the simplified arching analysis and the finite element analysis indicate that, although the side wall friction does affect the soil and pipe response, the influence over the range of values expected in the laboratory with successful boundary treatment is relatively small. Thus, levels of side wall friction less than 5° would not be expected to introduce a significant deviation from expected field conditions. It is also notable that the effort to obtain very low ϕ_{sw} (i.e., $\phi_{sw} \ll 5^\circ$) does not result in a substantial improvement in the laboratory idealization.

Influence of lateral boundary stiffness on soil and pipe response

All preceding analysis of the influence of the proximity and roughness of the lateral boundary of the test cell has assumed rigid side walls. Outward movements of the lateral boundary may alter the stress conditions within the ground and the pipe. Reductions in horizontal stresses, similar to those which occur behind a retaining wall when subject to

Fig. 12. Calculated vertical σ_y and horizontal σ_x stresses with depth 0.075 m away from the lateral boundary when subject to a vertical surcharge of 1000 kPa with different values of side wall friction ϕ_{sw} .



outward deformation, are expected with outward lateral deformations of the side walls. It is also expected that the impact of lateral deformations increases as the soil stiffness increases.

Results from two-dimensional finite element analysis are examined to obtain a measure of the impact of lateral boundary deformations on the soil and pipe response. The finite element mesh of Fig. 10 was used with the same soil and pipe constitutive parameters as previously described. Side wall friction of 5° was considered. The normal stiffness of the joint elements along the lateral boundary was varied to provide different magnitudes of outward lateral movement along the side wall (δ_x in Fig. 1c).

Soil response

Figure 14 shows the effect of lateral boundary stiffness on soil stresses. Vertical (σ_y) and horizontal (σ_x) stresses near the pipe ($x = 0.2$ m, $y = 0.8$ m) and close to the side wall ($x = 0.925$ m, $y = 0.8$ m) are reported for different magnitudes of lateral deflection ϕ_{sw} calculated at mid-depth along the side wall (i.e., $x = 1.0$ m, $y = 0.8$ m). Results are shown for deflections ranging from 0 to 7.5 mm of outward

Fig. 13. Vertical (a) and horizontal (b) stresses calculated in the soil when subject to a vertical surcharge of 1000 kPa with interface friction ϕ_{sw} of 5°.

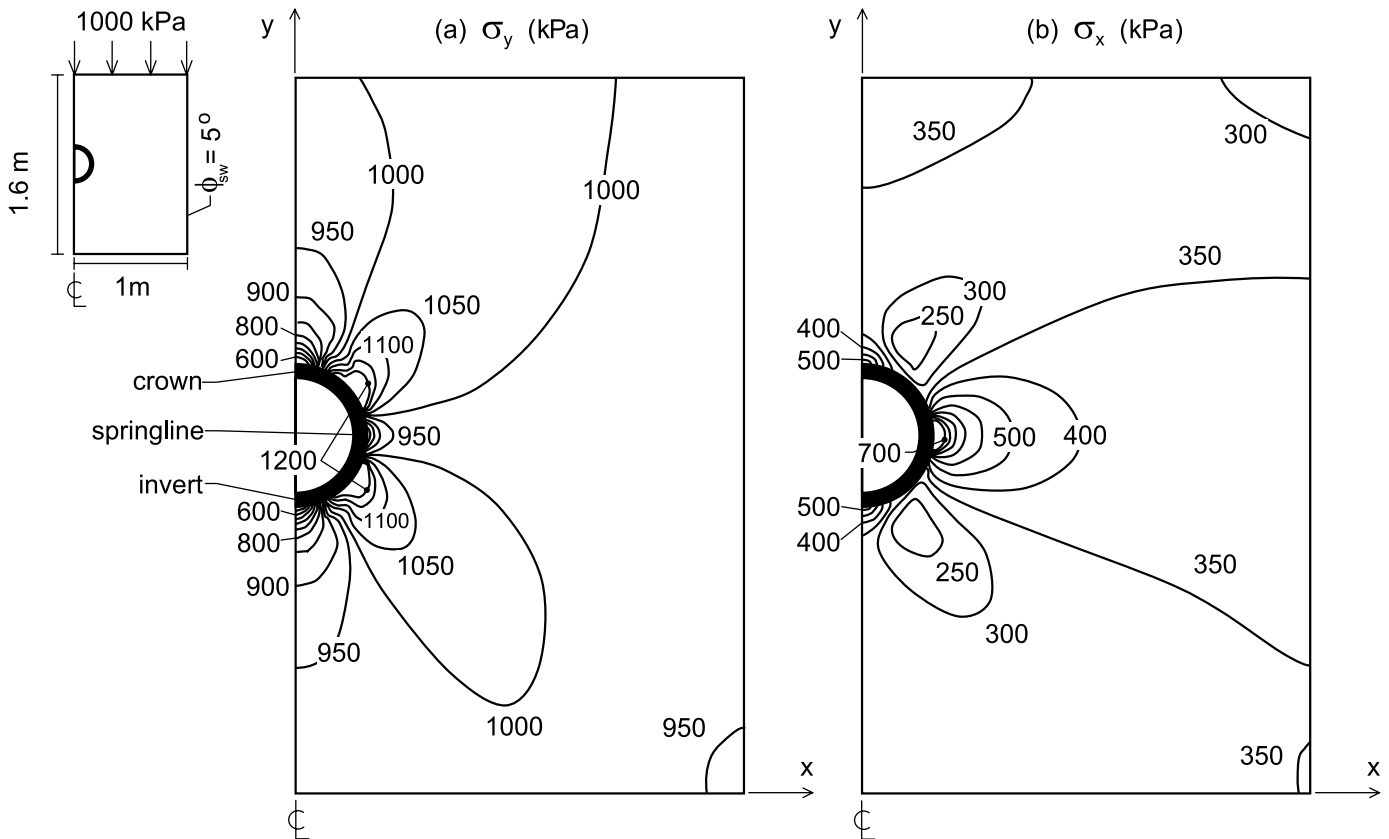


Table 1. Calculated pipe deflections (mm) at the crown (δ_{cr}), invert (δ_{in}), and spring line (δ_{sp}) and changes (mm) in vertical (ΔD_v) and horizontal (ΔD_h) pipe diameter for various levels of side wall friction ϕ_{sw} .

ϕ_{sw} (°)	δ_{cr}	δ_{in}	δ_{sp}	ΔD_v	ΔD_h
0	-10.9	-5.91	0.804	-4.99	1.61
5	-10.8	-5.78	0.818	-5.02	1.64
10	-10.6	-5.67	0.831	-4.93	1.66
24	-10.2	-5.37	0.868	-4.83	1.74
35	-9.91	-5.13	0.907	-4.78	1.84

movement (0–0.75% lateral strain) when subject to 1000 kPa vertical surcharge.

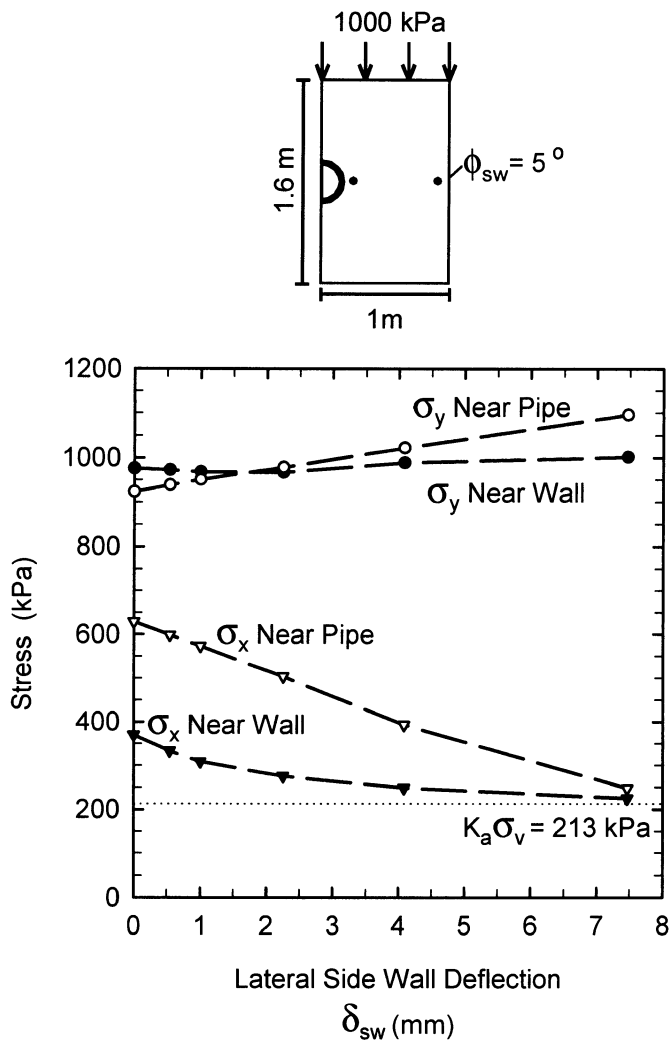
The vertical stresses calculated at mid-depth ($y = 0.8$ m) and near the wall are not greatly influenced by the magnitude of side wall deflection. At this location, the horizontal stresses are more sensitive to increases in lateral deflections, as horizontal stresses decrease with increasing side wall deflection. Near the side wall, horizontal stresses are 370 kPa for a rigid boundary and decrease to 225 kPa for boundary deflections of 7.5 mm, where active stress conditions are nearly mobilized. For larger deflections, horizontal stresses are limited by $K_a\sigma_y$, where an estimate of K_a may be given by Coulomb’s active earth pressure coefficient. For ϕ equal to 40°, side wall friction of 5°, and using the one-dimensional vertical stress results in the active limit of ap-

proximately 213 kPa. The results from the finite element analysis tend towards this limit. Lateral deflection of 1 mm leads to a 16% decrease in σ_x at this location (relative to rigid walls). For soil modulus of 50 MPa, the horizontal stress near the wall is reduced by 10% relative to rigid walls for side wall deflections of 1 mm. Impacts of boundary deformation are therefore more pronounced as the soil tested is stiffer. Selection of modulus of 80 MPa likely represents an upper estimate of the stiffness of ground materials to be tested in the facility. For tests involving ground materials to simulate burial conditions in landfills, values of soil modulus are expected to be less than 50 MPa. Hence the actual impact of the stiffness of the boundary in the new test cell is expected to be less than that reported here.

Stresses closer to the pipe are also influenced by the boundary stiffness. For rigid side walls horizontal stresses near the pipe are about 620 kPa (Fig. 14). Again, for δ_{sw} greater than 7.5 mm, horizontal stresses are close to active pressure conditions. There is little change in the vertical stress closer to the wall at this location. The selection of soil modulus has a greater effect on the stresses calculated near the pipe (compared with values near to the wall) given the close proximity of the zone of stress redistribution around the pipe which is influenced by the soil modulus.

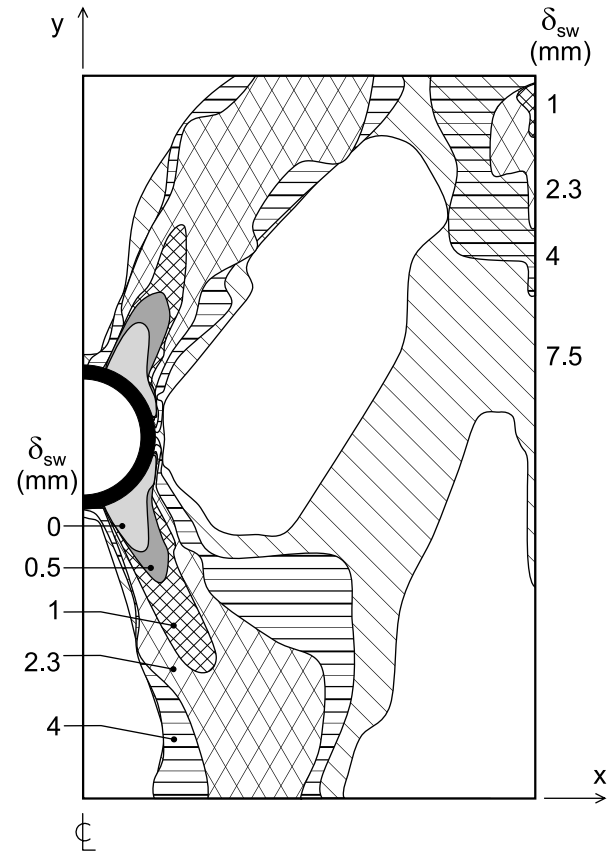
Zones of soil failure within the ground also depend on the lateral boundary stiffness. Figure 15 shows the location of zones of shear failure in the soil calculated for different magnitudes of side wall deflection. When the lateral

Fig. 14. Vertical σ_y and horizontal σ_x stresses calculated at mid-depth near the pipe and near the side wall for increasing lateral boundary deformation δ_{sw} when subject to a vertical surcharge of 1000 kPa with interface friction ϕ_{sw} of 5° .



boundaries are rigid, two local regions of soil failure occur near the pipe, namely at the shoulder and the haunch. This local plastic region occurs as the ratio of σ_1/σ_3 reaches N_ϕ at these locations (where $N_\phi = (1 + \sin \phi)/(1 - \sin \phi)$ for the frictional material modelled). Such soil failure is consistent with that described by Moore and Booker (1987) and leads to stress redistribution from the plastic to elastic material and increased stresses and deflections of the pipe. This is expected to occur under field conditions and is important to be able to simulate in the laboratory model. However, as the outward lateral deformation increases, these plastic regions extend farther out from the pipe, and extend towards the surface and base for deflections larger than 2 mm. Another local zone of soil failure appears near the outer top surface for lateral boundary deflections larger than 1 mm. When active conditions are approached (i.e., $\phi_{sw} = 7.5^\circ$), there is a significant region of soil failure corresponding to the large boundary deformations. Therefore, it is important to limit the boundary deflections to minimize the deviation in ground response from that expected to occur in the field.

Fig. 15. Calculated zones of shear failure in the soil for various lateral boundary deformations δ_{sw} when subject to a vertical surcharge of 1000 kPa with interface friction ϕ_{sw} of 5° .



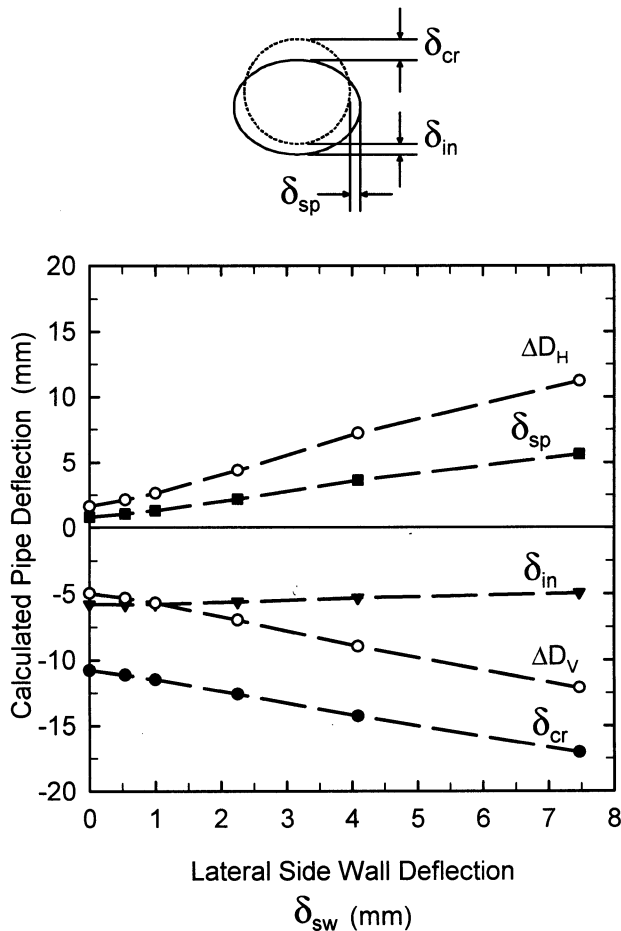
Pipe response

Clearly, there is a pronounced effect of lateral boundary stiffness on the soil response. Consequently the pipe response (deflections and stresses) is also significantly impacted by boundary deflections.

Calculated pipe deflections are plotted in Fig. 16 against the side wall deflection at a surcharge pressure of 1000 kPa. Crown deflections δ_{cr} increase while invert δ_{in} deflections decrease for increases in side wall deflection. This leads to an overall increase in the vertical diameter change ($\Delta D_v = \delta_{cr} - \delta_{in}$). Horizontal deflections at the spring line also increase for larger δ_{sw} , producing greater horizontal pipe diameter change ($\Delta D_h = 2 \delta_{sp}$). For boundary deformation of 1 mm at a vertical surcharge of 1000 kPa, ΔD_v is 1.14 times larger than that for rigid walls and ΔD_h is 1.6 times larger. For soil modulus of 50 MPa, increases in vertical and horizontal diameter change of 1.09 and 1.3 times relative to rigid walls were calculated.

As the side wall deflections increase, the decrease in lateral support for the pipe alters the mode of pipe deflection. This leads to greater bending stresses within the pipe relative to those calculated for rigid walls. The pipe experiences greater tensile stresses at the interior crown and invert locations, and there are greater compressive stresses at the interior spring line.

Fig. 16. Calculated pipe deflections at the crown, invert, and spring line (δ_{cr} , δ_{in} , and δ_{sp} , respectively) and vertical and horizontal diameter changes (ΔD_v and ΔD_h , respectively) for increasing lateral boundary deformation δ_{sw} when subject to a vertical surcharge of 1000 kPa with interface friction ϕ_{sw} of 5°.



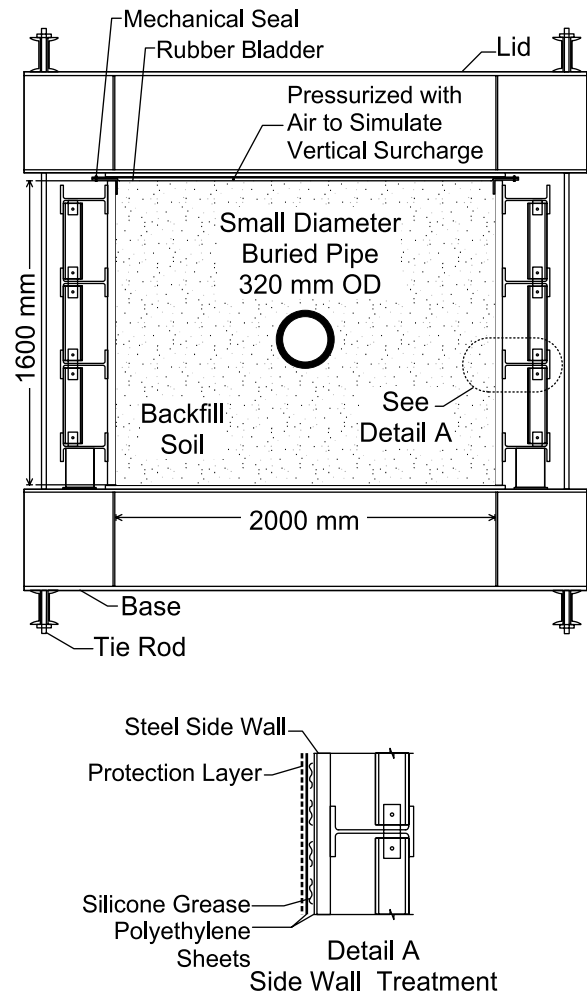
Since boundary deformations lead to pipe deflections and stresses that are larger than those expected for rigid walls, the pipe response measured in the new facility is likely to be more severe than the behaviour expected under deep and extensive overburden pressures (i.e., the measured pipe deflections and stresses are larger than would be expected under conditions of zero lateral strains). Limiting boundary deflections to 1 mm at a vertical surcharge of 1000 kPa results in a reasonable representation of the soil and pipe response under deep burial conditions.

Test cell design

The analyses reported in this paper assessing the effects of proximity, roughness, and stiffness of the lateral boundary were used to establish design limits for a new laboratory facility for testing small-diameter pipes when deeply buried under large overburden stresses.

A schematic drawing of the test cell is shown in Fig. 17. Inside dimensions are 2.0 m wide, 2.0 m long, and 1.6 m high. The test facility is self-equilibrated under the 4 MN applied force acting over 4.0 m² by tying the lid and base units together with twelve 25 mm diameter steel rods. The

Fig. 17. Transverse section through biaxial compression testing facility.



stiff side walls consist of four frames welded to 40 mm thick steel plates. This arrangement limits lateral deflections to 1 mm under 1000 kPa surcharge pressure in the bladder and for *K* of 0.5. Over a length of 2 m, this represents lateral deflections of less than two one-thousandths of the span (lateral soil strain $\epsilon_z < 0.1\%$).

Side wall friction treatment consisting of layers of polyethylene sheets lubricated with silicone grease is employed, limiting side wall friction to less than 5°. Protection of the interface is necessary and achieved with a 2 mm thick polyethylene sheet with horizontal slots (5 mm wide) to permit progressive shear failure to mobilize from the top downwards during testing (see Tognon et al. 1999).

Summary and conclusions

The design of a new laboratory facility for evaluating the performance of small-diameter pipes when buried under deep and extensive overburden material was presented. The facility involves a prism of soil with a pipe buried within, subject to large vertical pressures, while allowing only small horizontal deflections along the lateral boundaries. Attention focussed on the influence of the boundary conditions in the new facility and how reasonably the test cell represents the

field conditions for a buried pipe. Issues such as the loading conditions under deep burial, simulation of vertical earth pressures, development of lateral earth pressures, selection of test cell dimensions, and influence of sidewall friction and boundary stiffness on soil and pipe response were discussed.

(1) *Laboratory model*: The deep burial response of buried pipes is simulated in the laboratory by applying vertical and horizontal stresses on soil boundaries distant from the pipe. Vertical stresses that represent the weight of the overburden material above the deeply buried pipe are simulated with a uniformly distributed pressure at the surface of the test cell. A pressurized flexible membrane is used to apply the vertical pressure. Lateral stresses in the ground are developed by limiting the outward deflection of the boundaries.

(2) *Test cell dimensions*: Modified arching theory was used to provide a preliminary assessment of proximity and roughness of the lateral boundaries. The proportion of the vertical stress acting in the middle of the test cell increased as the distance to the boundary increased and the roughness of the boundary decreased. A practical limit was found where further increases in test cell dimensions resulted in only slight increases in the stresses acting within the ground. From these calculations and also considering the cost of test cell fabrication and the logistics of test cell use, dimensions with height of 1.6 m, breadth of 2.0 m, and length of 2.0 m were selected. It is expected that pipes up to an external diameter of 500 mm may be tested with minimal impact from the lateral boundaries. Negligible boundary impact is expected for pipes with external diameters less than 300 mm (e.g., most leachate collection pipes).

(3) *Boundary friction*: Finite element analysis was used to study the effects of boundary roughness on the response of the soil and pipe in the facility. Redistribution of stresses (relative to smooth boundaries) occurs within the ground caused by shear stresses mobilized along the boundaries. Vertical stresses decrease, and there are zones of both increasing and decreasing horizontal stresses within the ground. Maximum impact for untreated side walls may result in only 83% of the vertical stress and 60% of the horizontal stress relative to smooth boundaries. Caution should therefore be exercised with the interpretation of tests that involve only limited treatment or untreated boundaries. Effective treatment of the lateral boundary with lubricated polyethylene sheets can reduce side wall friction to less than 5°, resulting in less than 2% difference in vertical stresses throughout most of the stress field and only minimal impact on the pipe.

(4) *Boundary stiffness*: Finite element analysis was also conducted to examine the impact of lateral boundary deformations on the soil and pipe response. Outward movements of the lateral boundary may alter the stress conditions within the ground and the pipe. Horizontal stresses in the ground decreased as the side wall deflection increased, and the impact was pronounced for stiffer soils. For soil modulus of 50 MPa, the horizontal stress near the wall is reduced by 10% relative to that of rigid walls for side wall deflections of 1 mm. The reduced lateral stresses in the soil lead to larger vertical and horizontal diameter changes of the pipe which produce greater bending stresses within the pipe relative to those calculated for rigid walls. Since boundary de-

formations lead to pipe deflections and stresses which are larger than those expected for rigid walls, the pipe response measured in the new facility is likely to be more severe than the behaviour expected under deep and extensive overburden pressures. However, excessive boundary deformations may significantly change ground response and it is important to limit the boundary deflections to obtain lateral earth pressures close to those expected in the field.

(5) *New University of Western Ontario pipe testing facility*: Based on a series of finite element analyses, it is concluded that the test cell is expected to provide a reasonable simulation of the stress state for a pipe deeply buried under an embankment or landfill. Reduction of side wall friction to less than 5° (by inclusion of sheets of polyethylene lubricated with silicone grease) results in minimal changes relative to frictionless conditions. Specifications of structural stiffness are made to limit lateral boundary deformation to 1 mm at an applied surcharge of 1000 kPa. This ensures lateral earth pressures are within 10% of those expected in the field.

Acknowledgements

This work has been supported by the Natural Sciences and Engineering Research Council of Canada through research funds granted to Dr. Ian D. Moore and Dr. R. Kerry Rowe, as well through a PGS-B Scholarship awarded to Dr. Richard Brachman.

References

- Bathurst, R.J., and Benjamin, D.J. 1988. Preliminary assessment of side wall friction on large scale models in the RMC test facility. *In* The application of polymeric reinforcement in soil retaining structures. *Edited by* P.M. Jarrett and A. McGown. Kluwer Academic Publishers, Dordrecht, The Netherlands, pp. 181-192.
- Brachman, R.W.I. 1997. Hoop compression testing of HDPE leachate collection pipe. *In* Proceedings of Geosynthetics '97, Industrial Fabrics Association International (IFAI), Long Beach, Calif., pp. 337-350.
- Brachman, R.W.I. 1999. Mechanical performance of landfill leachate collection pipes. Ph.D. thesis, The University of Western Ontario, London, Ont.
- Brachman, R.W.I., Moore, I.D., and Rowe, R.K. 1996. Interpretation of a buried pipe test: small diameter pipe in the Ohio University facility. *Transportation Research Record* 1541, Structures, Culverts, and Tunnels. pp. 64-70.
- Brachman, R.W.I., Rowe, R.K., Moore, I.D., Tognon, A. 1998. Laboratory investigation of the performance of leachate collection pipe with coarse stone. *In* Proceedings of the 6th International Conference on Geosynthetics, Atlanta, Ga., pp. 191-196.
- Davis, E.H. 1969. Theories of plasticity on the failure of soil masses. *In* Soil mechanics selected topics. *Edited by* I.K. Lee. Butterworth, London, pp. 341-374.
- DiFrancesco, L.C., Selig, E.T., and McGrath, T.J. 1994. Laboratory testing of high density polyethylene drainage pipes. *Geotechnical Report* CPP93-412F, Department of Civil Engineering, University of Massachusetts at Amherst, Amherst, Mass.
- Höeg, K. 1968. Stresses against underground structural cylinders. *Journal of the Soil Mechanics and Foundation Division, ASCE*, 94(SM4): 833-858.
- Kastner, R.E., Sargand, S.M., and Mitchell, G.F. 1993. Structural performance of PVC leachate collection pipe. *In* Structural

- performance of pipes. *Edited by* S.M. Sargand, G.F. Mitchell, and J.O. Hurd. A.A. Balkema, Rotterdam, The Netherlands, pp. 83–95.
- Moore, I.D. 1993. Structural design of profiled polyethylene pipe. Part I. Deep burial. Geotechnical Research Centre Report GEOT-8-93, The University of Western Ontario, London, Ont.
- Moore, I.D., and Booker, J.R. 1987. Ground failure around buried tubes. *Rock Mechanics and Rock Engineering*, **20**: 243–260.
- Moore, I.D., and Hu, F. 1995. Response of HDPE pipe under hoop compression. *Transportation Research Record 1541, Structures, Culverts, and Tunnels*, pp. 29–36.
- Moore, I.D., and Laidlaw, T.C. 1997. Corrugation buckling in HDPE pipes — measurements and analysis. *In Proceedings of the 76th Annual Meeting of the Transportation Research Board*, Washington, D.C., January 11–15. Transportation Research Board Preprint 97-0565.
- Moore, I.D., Laidlaw, T.C., and Brachman, R.W.I. 1996. Test cells for static pipe response under deep burial. *In Proceedings of the 49th Canadian Geotechnical Conference*, September 23–25, St. John's, Nfld., pp. 737–744.
- Perloff, W.H., and Baron, W. 1976. *Soil mechanics principles and applications*. John Wiley & Sons, New York.
- Rogers, C.D.F., Fleming, P.R., and Talby, R. 1996. Use of visual methods to investigate the influence of installation procedure on pipe–soil interaction. *Transportation Research Record 1541, Structures, Culverts, and Tunnels*, pp. 76–85.
- Selig, E.T., DiFrancesco, L.C., and McGrath, T.J. 1994. Laboratory test of buried pipe in hoop compression. *In Buried plastic pipe technology*. Vol. 2. American Society for Testing and Materials, Special Technical Publication STP 1222, pp. 119–132.
- Tognon, A.R., Rowe, R.K., and Brachman, R.W.I. 1999. Evaluation of sidewall friction for a buried pipe testing facility. *Geotextiles and Geomembranes*, **17**: 193–212.
- Zanzinger, H., and Gartung, E. 1995. Large-scale model tests of leachate collection pipes in landfills under heavy loads. *In Advances in underground pipeline engineering*. *Edited by* J.K. Jeyapalan and M. Jeyapalan. American Society of Civil Engineers, New York, pp. 114–125.
- Zanzinger, H., and Gartung, E. 1998. HDPE-geopipes, soil–structure interaction. *In Proceedings of the 6th International Conference on Geosynthetics*, Atlanta, Ga., pp. 197–200.
- Zhang, C., and Moore, I.D. 1997. Finite element modelling of inelastic deformation of ductile polymers. *Geosynthetics International*, **4**(2): 137–163.